CHAPTER 3

QUANTUM CASCADE LASER

3.1 HETEROSTRUCTURES

3.1.1 Finite potential well

A **quantum well structure** is formed when the motion of electrons is confined in one direction (e.g., the x direction), while remaining free in the other two dimensions (y, z).

This situation is achieved by placing a layer of semiconductor crystal between two layers of another semiconductor, so that the **profile of the conduction band edge Ec forms a potential well**.

The electrons are **confined in one direction** within the region $0 < x < a$. Let us denote by U_0 the height of the potential barrier, assumed to be finite.

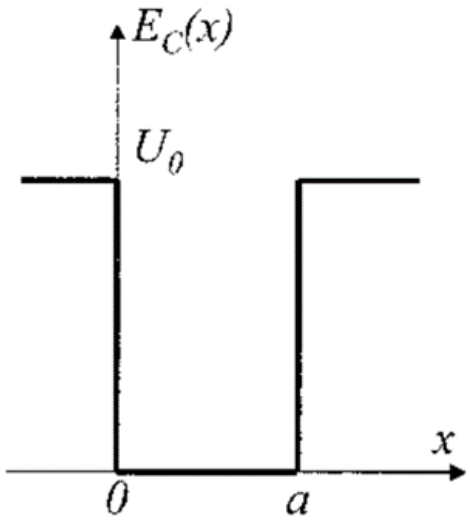

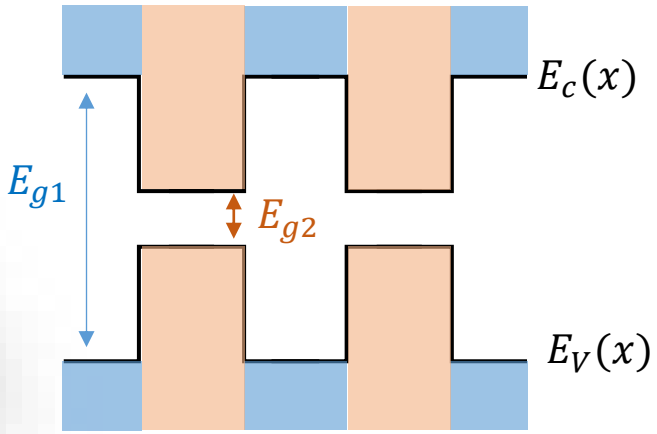

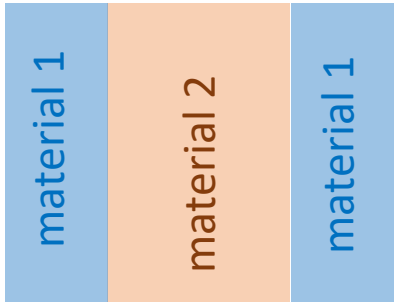

3.1 HETEROSTRUCTURES

3.1.1 Finite potential well

The energy bands can be derived by considering the motion of electrons in the heterostructure.

The effect of the periodic crystal potential will be taken into account by introducing the **effective mass** of the electron.

The potential in the x direction is analogous to that of a particle in a finite potential well. The height of the potential barrier is given by the difference between the conduction band edges of the two semiconductors, commonly referred to as the **band offset**.

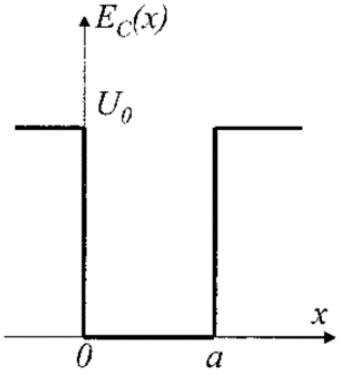

The contribution of this potential in the other two directions (y, z) is constant and can therefore be set to zero, similarly to the case of a free particle.

The potential can therefore be expressed as:

$$U(x,y,z) = \begin{cases} 0 & \text{se } 0 < x < a \\ U_0 > 0 & \text{se } x < 0 \text{ e } x > a \end{cases}$$

3.1 HETEROSTRUCTURES

3.1.1 Finite potential well

The Schrodinger equation is:

$$-\frac{\hbar^2}{2m^*}\nabla^2\Psi(x,y,z) - [E - U(x,y,z)]\Psi(x,y,z) = 0$$

$$U(x,y,z) = \begin{cases} 0 & \text{se } 0 < x < a \\ U_0 > 0 & \text{se } x < 0 \; e \; x > a \end{cases}$$

where m^* is the effective mass of the electron.

The shape of the potential suggests that the motion along the x direction and in the (y,z) plane are independent.

It is common to introduce the subscript $\perp$ to indicate the motion and energies along the x direction and the subscript $//$ to indicate the motion and energies in the (y,z) plane.

The wavefunction solution to the Schrodinger equation can be written as the product of two functions: one depending only on x, and the other on the (y,z) directions.

$$\Psi(x,y,z) = \Psi_{//}(\overrightarrow{r_{//}})\Psi_{\perp}(\overrightarrow{r_{\perp}})$$

and the energy spectrum can be expressed as the sum of two independent contributions:

$$E(\vec{k}) = \mathrm{E}_{//}(\overrightarrow{k_{//}}) + \mathrm{E}_{\perp}(\overrightarrow{k_{\perp}})$$

3.1 HETEROSTRUCTURES

3.1.1 Finite potential well

Let's analyze the two contributions separately.

In the (y,z) plane, the motion of the electron is similar to that of a free particle. The wavefunction $\Psi_{//}(\overrightarrow{r_{//}})$ can be considered as a plane wave:

$$\Psi(x,y,z) = \Psi_{//}(\overrightarrow{r_{//}})\Psi_{\perp}(\overrightarrow{r_{\perp}})$$

$$E(\vec{k}) = \mathrm{E}_{//}(\overrightarrow{k_{//}}) + \mathrm{E}_{\perp}(\overrightarrow{k_{\perp}})$$

$$\Psi_{//}(\overrightarrow{r_{//}}) = Ae^{i\overrightarrow{k_{//}}\cdot\overrightarrow{r_{//}}}$$

where A is a normalization constant.

The related energy spectrum contribution is then:

$$\mathrm{E}_{//}(\overrightarrow{k_{//}}) = \frac{\hbar^2\overrightarrow{k_{//}^2}}{2m^*} = \frac{\hbar^2(k_y^2 + k_z^2)}{2m^*}$$

This treatment is valid only for small values of the momentum, that is, if $|\overrightarrow{k_{//}}| \ll |\vec{G}|$ where $\vec{G}$ is a reciprocal lattice vector.

This restriction considers the fact that the electron cannot be considered free, due to the presence of the crystal potential (**see the Kronig–Penney model**)

3.1 HETEROSTRUCTURES

3.1.1 Finite potential well

In the x direction, the discussion is identical to that of a particle in a finite potential well.

In such a potential, the Schrodinger equation becomes $\Psi_{\perp}(\overrightarrow{r_{\perp}}) = \Psi(x)$:

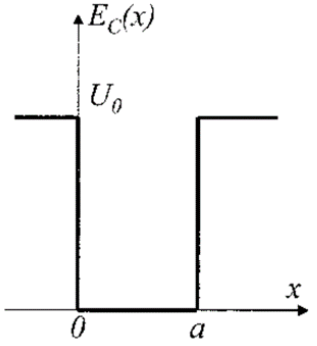

$$\begin{cases} \dfrac{\hbar^2}{2m^*}\dfrac{\mathrm{d}^2\Psi(x)}{\mathrm{dx}^2} + (E - U_0)\Psi(x) = 0 & \text{if } x < 0 \; e \; x > a \\ \dfrac{\hbar^2}{2m^*}\dfrac{\mathrm{d}^2\Psi(x)}{\mathrm{dx}^2} + E\Psi(x) = 0 & \text{if } 0 < x < a \end{cases}$$

Both cases must be resolved.

Let's write both equations in a more compact way by introducing:

$$-\frac{\hbar^2}{2m^*}\nabla^2\Psi(x,y,z) - [E - U(x,y,z)]\Psi(x,y,z) = 0$$

$$\begin{cases} \alpha = \sqrt{\dfrac{2m^*(U_0 - E)}{\hbar^2}} \\ k = \sqrt{\dfrac{2m^*E}{\hbar^2}} \end{cases} \Rightarrow \begin{cases} \dfrac{\mathrm{d}^2\Psi(x)}{\mathrm{dx}^2} - \alpha^2\Psi(x) = 0 & \text{if } x < 0 \; e \; x > a \\ \dfrac{\mathrm{d}^2\Psi(x)}{\mathrm{dx}^2} + k^2\Psi(x) = 0 & \text{if } 0 < x < a \end{cases}$$

3.1 HETEROSTRUCTURES

3.1.1 Finite potential well

The general solutions are:

$$\begin{cases} \Psi_-(x) = \mathrm{A}_- e^{\alpha x} + \mathrm{B}_- e^{-\alpha x} & \text{if } x < 0 \\ \Psi_0(x) = \mathrm{A}_0 sen(kx) + \mathrm{B}_0 cos(kx) & \text{if } 0 < x < a \\ \Psi_+(x) = \mathrm{A}_+ e^{\alpha x} + \mathrm{B}_+ e^{-\alpha x} & \text{if } x > a \end{cases}$$

$$\begin{cases} \frac{\mathrm{d}^2\Psi(x)}{\mathrm{dx}^2} - \alpha^2\Psi(x) = 0 \quad se\ x < 0\ e\ x > a \\ \frac{\mathrm{d}^2\Psi(x)}{\mathrm{dx}^2} + k^2\Psi(x) = 0 \quad se\ 0 < x < a \end{cases}$$

The **boundary conditions** impose:

1. $\Psi(x)$ must be finite as $x \to +\infty$ and $x \to -\infty$
2. The continuity of $\Psi(x)$ and its first derivative at the points $x = 0$ and $x = a$

$$\begin{cases} \Psi_-(-\infty) = 0 & \Psi_+(+\infty) = 0 \\ \Psi_-(0) = \Psi_0(0) & \Psi_0(a) = \Psi_+(a) \\ \frac{d\Psi_-(0)}{dx} = \frac{d\Psi_0(0)}{dx} & \frac{d\Psi_0(a)}{dx} = \frac{d\Psi_+(a)}{dx} \end{cases}$$

By solving these equations, the conditions can be made explicit:

$$\begin{cases} \mathrm{B}_- = 0 & \mathrm{A}_+ = 0 \\ \mathrm{A}_- = \mathrm{B}_0 & \mathrm{A}_0 sen(ka) + \mathrm{B}_0 cos(ka) = \mathrm{B}_+ e^{-\alpha a} \\ \alpha \mathrm{A}_- = kA_0 & k\mathrm{A}_0 cos(ka) - k\mathrm{B}_0 sen(ka) = -\alpha \mathrm{B}_+ e^{-\alpha a} \end{cases}$$

3.1 HETEROSTRUCTURES

3.1.1 Finite potential well

Combining $\mathrm{A}_- = \mathrm{B}_0$ and $\alpha \mathrm{A}_- = kA_0$, we get that $B_0 = \frac{k}{\alpha}\mathrm{A}_0$, which can be substituted into the remaining two equations:

$$\begin{cases} \mathrm{B}_- = 0 & \mathrm{A}_+ = 0 \\ \mathrm{A}_- = \mathrm{B}_0 & \mathrm{A}_0 sen(ka) + \mathrm{B}_0 cos(ka) = \mathrm{B}_+ e^{-\alpha a} \\ \alpha \mathrm{A}_- = kA_0 & k\mathrm{A}_0 cos(ka) - k\mathrm{B}_0 sen(ka) = -\alpha \mathrm{B}_+ e^{-\alpha a} \end{cases}$$

$$\begin{cases} A_0 \left[sen(ka) + \frac{k}{\alpha} cos(ka) \right] - \mathrm{B}_+ e^{-\alpha a} = 0 \\ A_0 \frac{k}{\alpha} \left[cos(ka) - \frac{k}{\alpha} \mathrm{sen}(ka) \right] + \mathrm{B}_+ \alpha e^{-\alpha a} = 0 \end{cases}$$

Summing the equations, we obtain the condition for a non-trivial solution:

$$sen(ka) + \frac{k}{\alpha} cos(ka) + \frac{k}{\alpha} \cos(ka) - \frac{k^2}{\alpha^2} \mathrm{sen}(ka) = 0$$

from which:

$$(k^2 - \alpha^2) sen(ka) - 2\alpha k cos(ka) = 0$$

that can be rewritten as:

$$tg(ka) = \frac{2\alpha k}{k^2 - \alpha^2}$$

3.1 HETEROSTRUCTURES

3.1.1 Finite potential well

Introducing the new constants:

$$\begin{cases} \alpha_0 = \sqrt{\dfrac{2m^* U_0}{\hbar^2}} \\ \varsigma = \dfrac{E}{U_0} \end{cases}$$

we can rewrite the two constants introduced above:

$$\begin{cases} \alpha = \alpha_0\sqrt{1-\varsigma} \\ k = \alpha_0\sqrt{\varsigma} \end{cases}$$

$$tg(ka) = \frac{2\alpha k}{k^2 - \alpha^2}$$

$$\alpha = \sqrt{\frac{2m^*(U_0 - E)}{\hbar^2}}$$

$$k = \sqrt{\frac{2m^* E}{\hbar^2}}$$

and so the boundary condition

$$tg(a\alpha_0\sqrt{\varsigma}) = \frac{2\sqrt{\varsigma(1-\varsigma)}}{2\varsigma - 1}$$

This equation has only one variable, ζ, and each value that satisfies it allows us to determine E, k, and α, and hence $\Psi(x)$, which is the solution of the Schrödinger equation for a finite potential well in the case$0 < E < U_0$.

This equation can be solved graphically. The intersection points correspond to the **number of bound states in the finite potential well**.

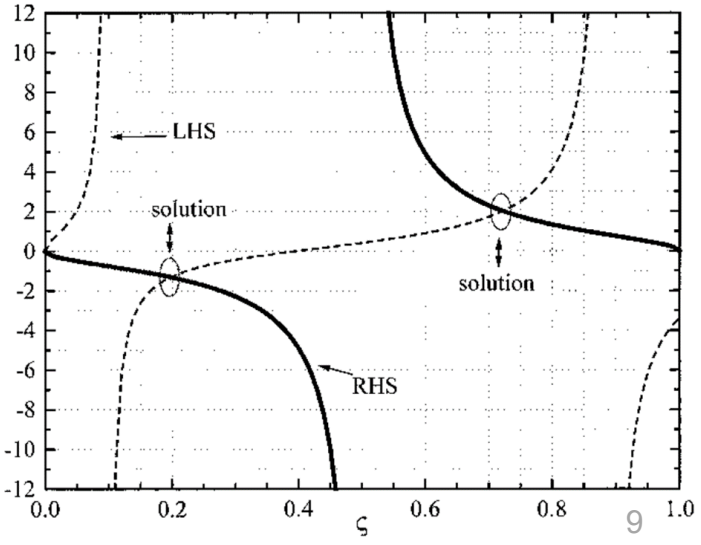

3.1 HETEROSTRUCTURES

3.1.2 Quantized energy levels

As the well height (U_0) increases, α_0 increases, the period of the function increases, and therefore decreases $tg(a\alpha_0\sqrt{\varsigma})$.

$$\alpha_0 = \sqrt{\frac{2m^* U_0}{\hbar^2}} \qquad \varsigma = \frac{E}{U_0}$$

It follows that a larger number of branches of tangent functions can be intercepted by the function $\frac{2\sqrt{\varsigma(1-\varsigma)}}{2\varsigma-1}$.

$$tg(a\alpha_0\sqrt{\varsigma}) = \frac{2\sqrt{\varsigma(1-\varsigma)}}{2\varsigma-1}$$

This means that the number of intersections increases.

Since there are only a discrete number of ς, this means that there are a **discrete number of energy values E**, and so the **energy levels are quantized**.

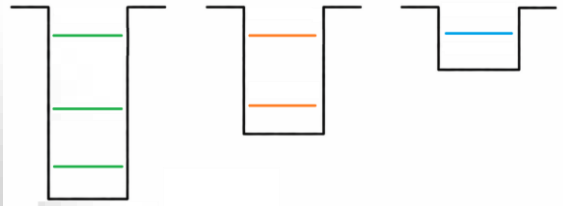

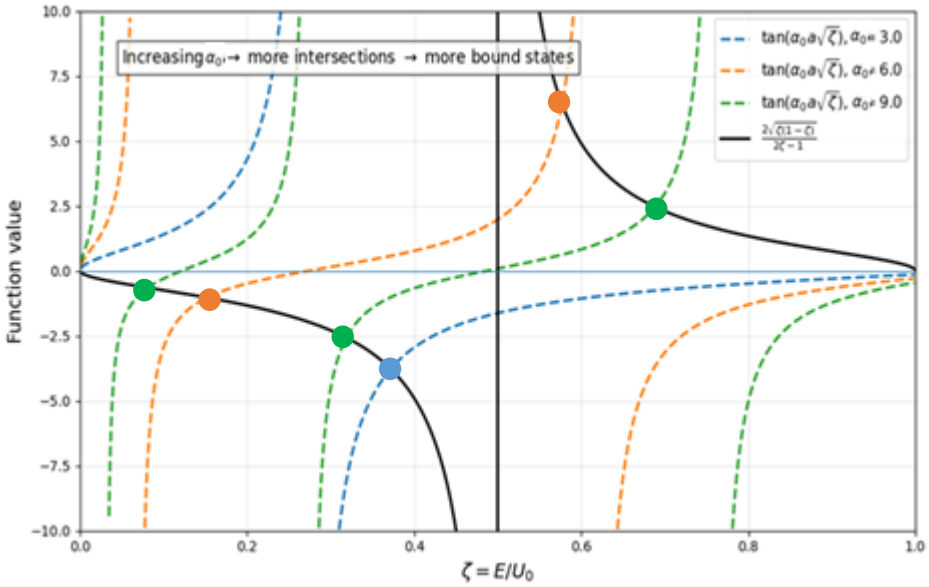

3.1 HETEROSTRUCTURES

3.1.2 Quantized energy levels

The discrete values of ζ_n lead to discrete values of k_n and α_n.

$$\begin{cases} \alpha_n = \alpha_0\sqrt{1-\zeta_n} \\ k_n = \alpha_0\sqrt{\zeta_n} \end{cases}$$

These quantities determine a discrete set of allowed energy levels $\mathrm{E}_{\perp,n}$

Each energy level $\mathrm{E}_{\perp,n}$ is associated with a corresponding wavefunction $\Psi_n(x)$.

$$k_n = \sqrt{\frac{2m^*\mathrm{E}_{\perp,n}}{\hbar^2}}$$

$$\alpha_n = \sqrt{\frac{2m(U_0 - \mathrm{E}_{\perp,n})}{\hbar^2}}$$

$$\Psi_n(x) = \begin{cases} \mathrm{A}_- e^{\alpha_n x} & se\ x < 0 \\ \mathrm{A}_0 sen(k_n x) + \mathrm{B}_0 sen(k_n x) & se\ 0 < x < a \\ \mathrm{B}_+ e^{-\alpha_n x} & se\ x > a \end{cases}$$

Inside the well, the wavefunction is oscillatory with a wavenumber k_n; outside the well, the wavefunction decays exponentially with a constant decay α_n.

The parameters k_n and α_n are quantized and share the same index n as the energy levels.

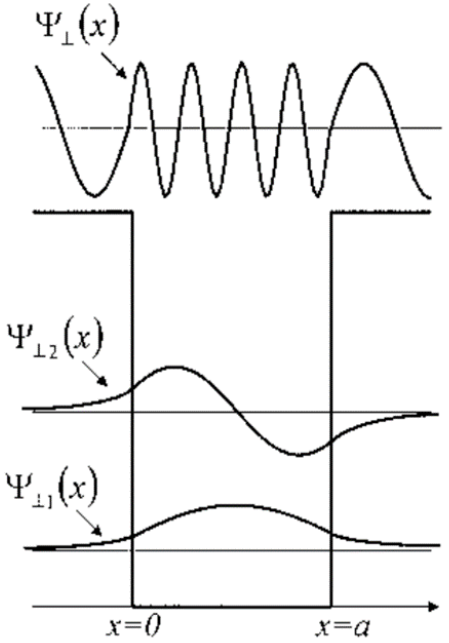

3.1 HETEROSTRUCTURES

3.1.2 Quantized energy levels

$$\mathrm{E}_{//}\left(\overrightarrow{k_{//}}\right) = \frac{\hbar^2 \overrightarrow{k_{//}^2}}{2m^*} = \frac{\hbar^2\left(k_y^2 + k_z^2\right)}{2m^*}$$

$$\alpha_n = \sqrt{\frac{2m\left(U_0 - \mathrm{E}_{\perp,n}\right)}{\hbar^2}}$$

The total energy spectrum of an electron in a heterostructure is given by:

$$E\left(\vec{k}, n\right) = \mathrm{E}_{//}\left(\overrightarrow{k_{//}}\right) + \mathrm{E}_{\perp,n} = \frac{\hbar^2 \vec{k}_{//}^2}{2m^*} + \mathrm{E}_{\perp,n}$$

The total energy is the sum of a **continuous contribution** (free motion in the (x,y) plane) and a **quantized contribution** (confinement along z).

Each level $\mathrm{E}_{\perp,n}$ forms a parabola as a function of $k_{//}$.

Each parabola is called **subband**.

The Figure shows a set of parabolic subbands, each corresponding to a quantized level E_n.

Radiative and no-radiative transitions can occur between these quantized subbands.

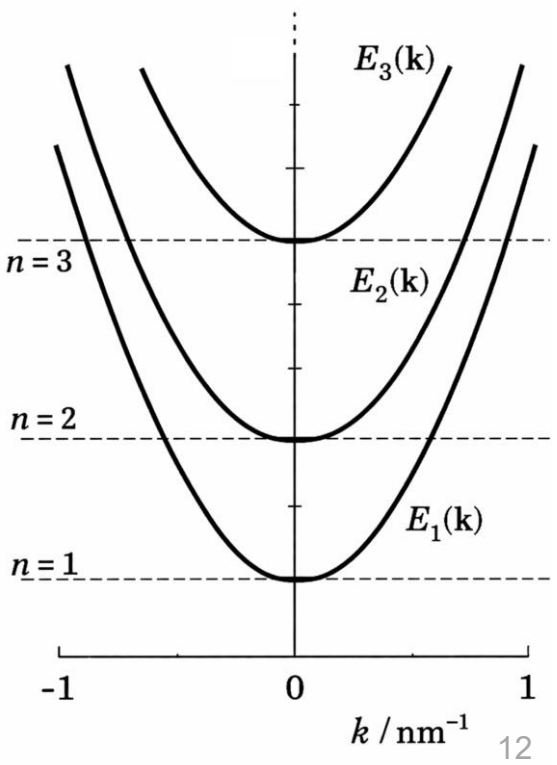

3.1 HETEROSTRUCTURES

3.1.3 Density of states

The density of states $g_{2D}(E)$ counts how many quantum states are available at a given energy E.

$$E(\vec{k},n)=\frac{\hbar^2\vec{k}_{//}^2}{2m^*}+\mathrm{E}_{\perp,n}$$

A convenient way to express this is to treat E as a continuous variable and sum over all states, indexed by the quantum number n and the in-plane wavevector $\overrightarrow{k_{//}}$.

Each state contributes only if its energy matches E, which is enforced by the Dirac delta function:

$$g_{2D}(E)=2\sum_{n,\overrightarrow{k_{//}}}\delta\left[\mathrm{E}_{//}\left(\overrightarrow{k_{//}}\right)+\mathrm{E}_{\perp,n}-E\right]$$

The factor 2 accounts for spin degeneracy.

Since $\overrightarrow{k_{//}}$ is continuous, the sum can be replaced by an integral over the 2D momentum space:

$$\sum_{\overrightarrow{k_{//}}}\rightarrow\frac{S}{(2\pi)^2}\int d\overrightarrow{k_{//}}$$

where $\frac{(2\pi)^2}{S}$ is the area of a single state in 2D k-space, and S is the area of the heterostructure in the real space.

3.1 HETEROSTRUCTURES

3.1.3 Density of states

Thus, $g_{2D}(E)$ becomes:

$$g_{2D}(E) = \frac{2S}{(2\pi)^2}\sum_n \int_{\overrightarrow{k_{//}}} \delta\left[\mathrm{E}_{//}\left(\overrightarrow{k_{//}}\right) + \mathrm{E}_{\perp,n} - E\right] d\overrightarrow{k_{//}}$$

$$g_{2D}(E) = 2\sum_{n,\overrightarrow{k_{//}}} \delta\left[\mathrm{E}_{//}\left(\overrightarrow{k_{//}}\right) + \mathrm{E}_{\perp,n} - E\right]$$

$$\sum_{\overrightarrow{k_{//}}} \rightarrow \frac{S}{(2\pi)^2}\int d\overrightarrow{k_{//}}$$

Let's differentiate the expression of $\mathrm{E}_{//}\left(\overrightarrow{k_{//}}\right)$:

$$d\left[\mathrm{E}_{//}\left(\overrightarrow{k_{//}}\right)\right] = \frac{\hbar^2}{2m^*}\left(2k_{//}\right)dk_{//}$$

$$\mathrm{E}_{//}\left(\overrightarrow{k_{//}}\right) = \frac{\hbar^2 \vec{k}_{//}^2}{2m^*}$$

where $k_{//}$ is the magnitude of the vector $\overrightarrow{k_{//}}$.

In two dimensions: $d\overrightarrow{k_{//}} = d\left(\pi {k_{//}}^2\right) = 2\pi k_{//} dk_{//}$

Substituting: $d\left[\mathrm{E}_{//}\left(\overrightarrow{k_{//}}\right)\right] = \frac{\hbar^2}{2m^*}\frac{1}{\pi}d\overrightarrow{k_{//}}$

Then, substituting into the expression for $g_{2D}(E)$:

$$g_{2D}(E) = \frac{2S}{(2\pi)^2}\left(\frac{2m^*\pi}{\hbar^2}\right)\sum_n \int_0^{+\infty} \delta\left[\mathrm{E}_{//}\left(\overrightarrow{k_{//}}\right) + \mathrm{E}_{\perp,n} - E\right] d\left[\mathrm{E}_{//}\left(\overrightarrow{k_{//}}\right)\right]$$

3.1 HETEROSTRUCTURES

3.1.3 Density of states

$$g_{2D}(E) = \frac{2S}{(2\pi)^2}\left(\frac{2m^*\pi}{\hbar^2}\right)\sum_n \int_0^{+\infty} \delta\left[\mathrm{E}_{//}(\overrightarrow{k_{//}}) + \mathrm{E}_{\perp,n} - E\right] d\left[\mathrm{E}_{//}(\overrightarrow{k_{//}})\right]$$

By introducing the variable $x = \mathrm{E}_{//}(\overrightarrow{k_{//}})$ the integral becomes:

$$g_{2D}(E) = \frac{Sm^*}{\pi\hbar^2}\sum_n \int_0^{+\infty} \delta\left[\mathrm{x} + \mathrm{E}_{\perp,n} - E\right] d\mathrm{x}$$

$$\Theta(\mathrm{x}) := \int_{-\infty}^{x} \delta(s)\, ds$$

The integral of the Dirac function is the Heaviside function:

Therefore: $$g_{2D}(E) = \frac{Sm^*}{\pi\hbar^2}\sum_n \Theta\left[E - \mathrm{E}_{\perp,n}\right]$$

This result shows that, in a quantum well, the density of states of quasi-two-dimensional electrons is a **step-like function of energy**. It increases by an amount $\frac{Sm^*}{\pi\hbar^2}$ each time the energy E crosses a quantized level $E_{\perp,n}$.

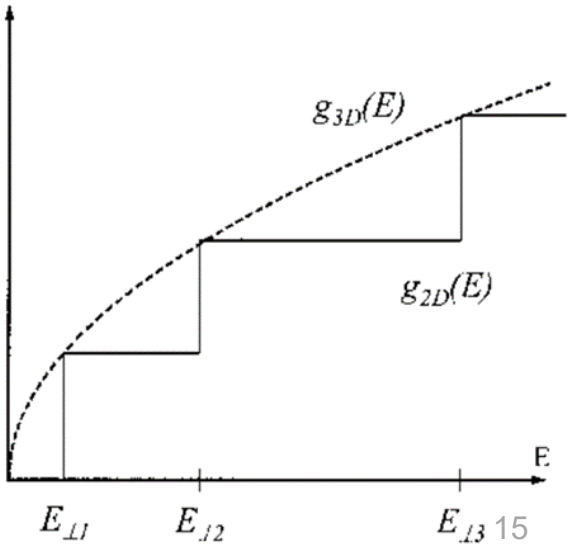

3.1 HETEROSTRUCTURES

3.1.3 Density of states

At each value of $\mathrm{E}_{\perp,n}$, a new energy subband begins.

The density of states within each subband is constant, resulting in a step-like structure.

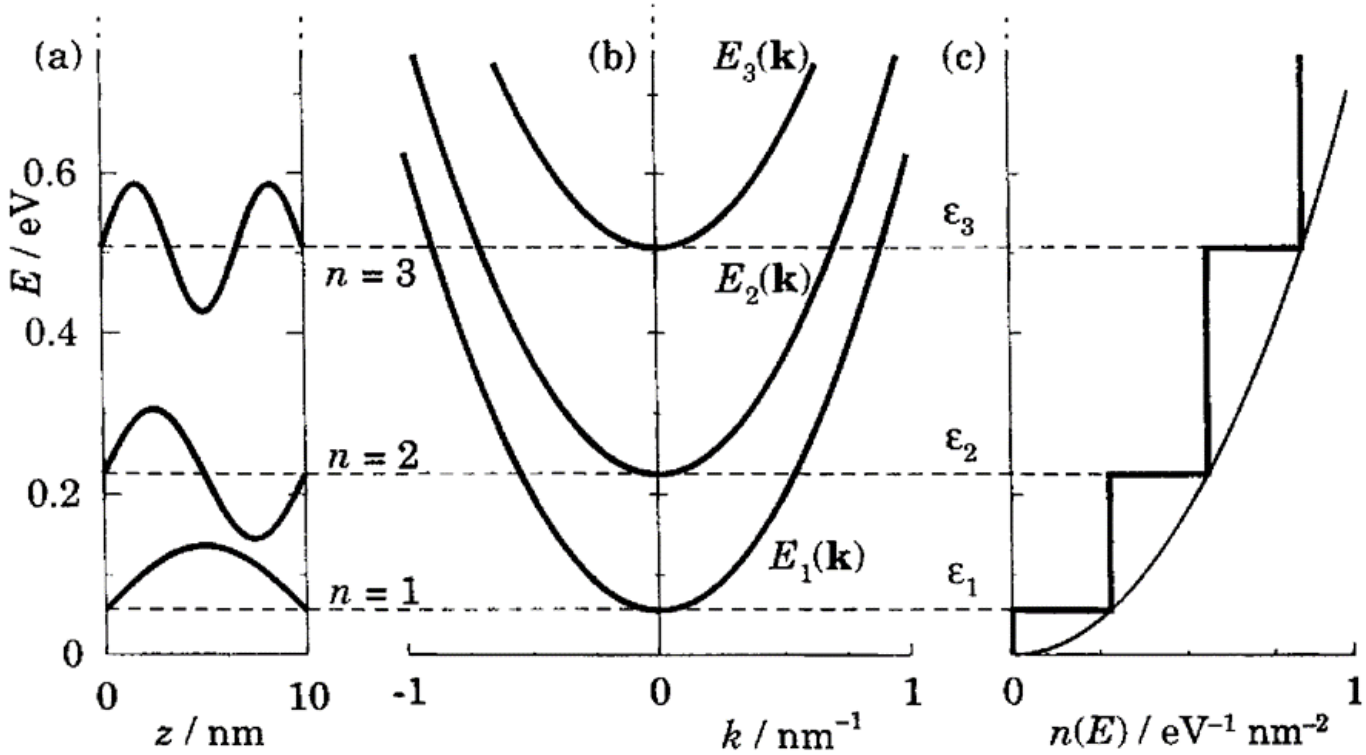

It can be shown that the density of states for a quasi-two-dimensional system exhibits discontinuities at the energies $\mathrm{E} = \mathrm{E}_{\perp,\mathrm{n}}$.

3.1 HETEROSTRUCTURES

3.1.3 Role of the effective mass

The difference in the density of states between a quantum well and a 3D structure reflects the different nature of electron motion.

Motion in the plane makes the density of states independent of the subband energy.

For motion perpendicular to the plane, a new quantum number n arises due to confinement along this direction.

Excitation of an electron in this direction increases the quantum number n, leading to a transition to a higher subband.

In previous discussion, for simplicity, we assumed a single value of the effective mass m^*.

Two different effective masses must be considered, one for each material.

In this case, the Schrödinger equation becomes:

$$\begin{cases} -\dfrac{\hbar^2}{2m_1{}^*}\nabla^2\Psi(x,y,z) - [E - U(x,y,z)]\Psi(x,y,z) = 0 & \text{if } x < 0 \; e \; x > a \\ -\dfrac{\hbar^2}{2m_2{}^*}\nabla^2\Psi(x,y,z) - [E - U(x,y,z)]\Psi(x,y,z) = 0 & \text{if } 0 < x < a \end{cases}$$

The boundary conditions must also be revised.

This refinement leads to a more accurate description, while leaving the main physical conclusions unchanged.

3.2 QUANTUM CASCADE LASERS

3.2.1 Long-wavelength approaches

Semiconductor laser diodes operate efficiently over a **limited spectral range** determined by the **bandgap of the material**.

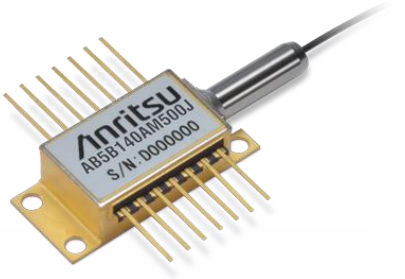

Typical emission wavelengths span **from the visible to the mid-infrared**

$$\lambda \approx 0.7\ \mu m \text{ to } 3.0\ \mu m$$

Different material systems are used to cover specific spectral regions.

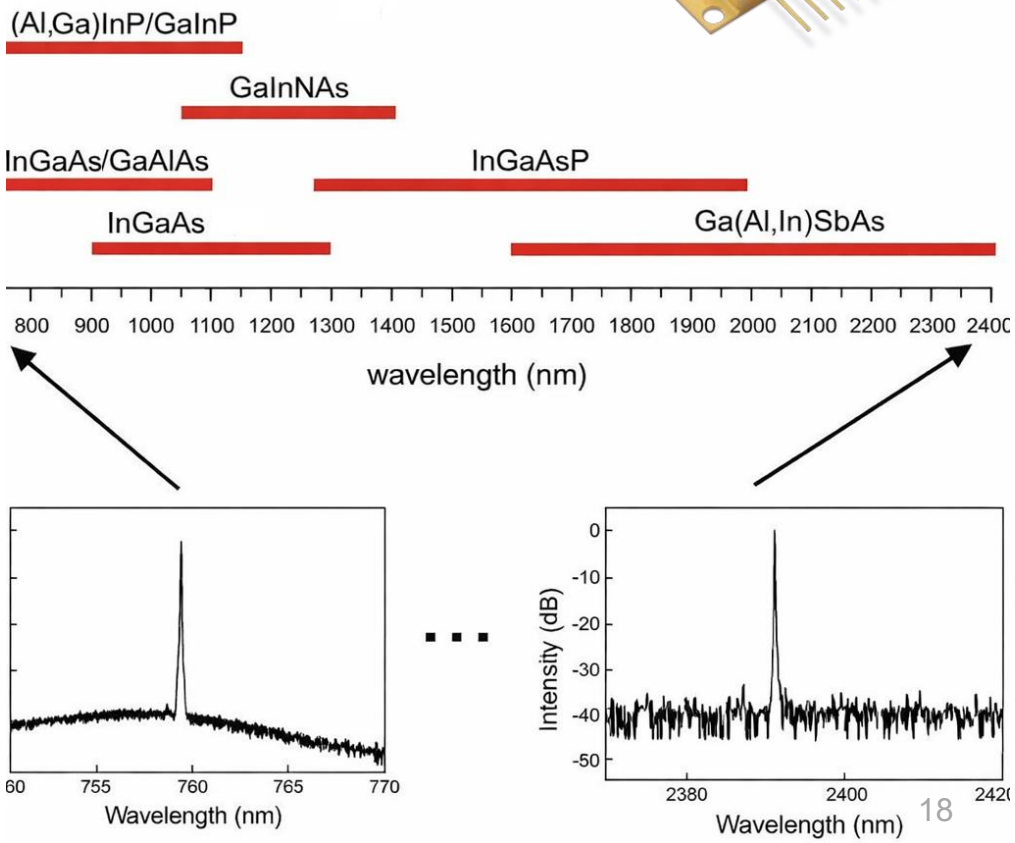

Semiconductor lasers that exploit direct transitions between the conduction and valence bands for photon emission are referred to as **interband lasers**.

Their efficient operation is **limited to wavelengths below ~ 3 µm**.

3.2 QUANTUM CASCADE LASERS

3.2.1 Long-wavelength approaches

The efficiency of interband semiconductor lasers decreases rapidly at longer wavelengths.

At longer wavelengths, one must utilize a **smaller bandgap semiconductors**, typically based on InGaSb/GaSb materials.

The main difficulty in realizing a diode laser that emits at room temperature at $\lambda > 3.0\ \mu m$ is the high rate of non-radiative recombination, dominated by **Auger recombination processes** , in narrow bandgap semiconductors.

In **Chapter 2**, we described the carrier recombination mechanisms by considering both radiative and non-radiative contributions.

$$R(n) = A_{nr}n + Bn^2 + Cn^3 + R_{st}N_{ph}$$

$$J_{th} = qdn_{th}(A_{nr} + Bn_{th} + Cn_{th}{}^2)$$

We then related these mechanisms to the threshold current density.

The last contribution is the Auger recombination, which was neglected in **Chapter 2**.

When this term is no longer negligible, it significantly increases the threshold condition. As a result, higher carrier densities are required to achieve population inversion.

If dominant, it prevents the achievement of sufficient gain for stimulated emission.

3.2 QUANTUM CASCADE LASERS

3.2.2 Auger recombination

In an Auger recombination process, the energy released by the recombination of an electron–hole pair is not emitted as a photon but is **transferred to a third carrier** (electron in the Figure) via scattering processes.

This third carrier is excited to a higher energy state within the conduction band, as schematically shown in the Figure.

Since no photons are generated, Auger recombination represents a non-radiative loss mechanism.

The Auger recombination rate **depends critically on the bandgap energy**:

$$R_{Auger} \propto n^3 e^{-E_g/kT}$$

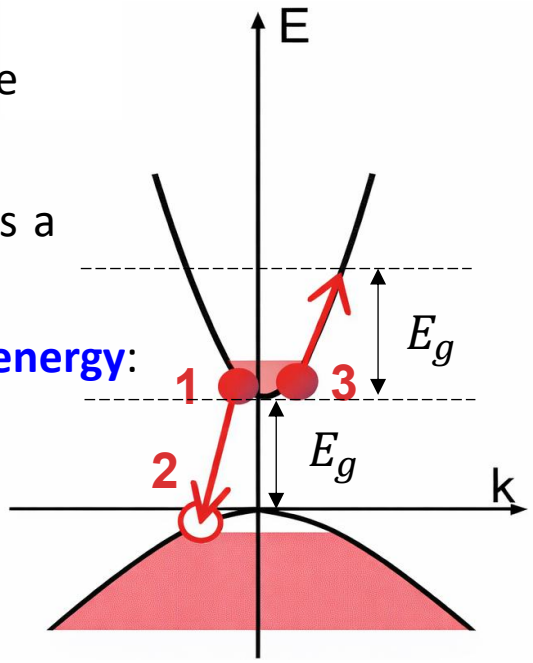

The exponential dependence can be intuitively understood by considering the **energy distribution of carriers in the conduction band**.

As E_g decreases, the high-energy tail of the carrier distribution ($f(E) \sim e^{-E/kT}$) becomes sufficient to populate states in conduction band (electron 1 and 3), leading to an exponential increase of Auger recombination.

3.2 QUANTUM CASCADE LASERS

3.2.2 Auger recombination

Therefore, by choosing materials with a narrow bandgap to achieve longer emission wavelengths, Auger recombination inevitably becomes dominant.

As a result, the device efficiency decreases significantly, particularly in terms of emitted optical power, since radiative transitions are overwhelmed by non-radiative Auger processes.

A possible solution is to exploit optical transitions between quantized electronic states (**subbands**) created by spatial confinement in semiconductor heterostructures.

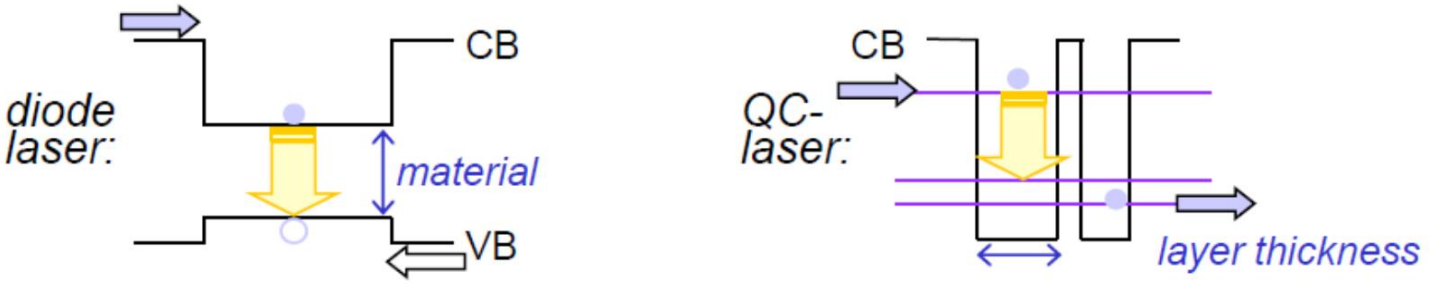

In **intersubband transitions**, only electrons are involved, eliminating electron–hole recombination and strongly reducing Auger processes.

Semiconductor lasers that rely on intersubband transitions within the conduction band are known as **quantum cascade lasers**.

3.2 QUANTUM CASCADE LASERS

3.2.3 From the cascade scheme to the quantum cascade laser

The starting point is a planar semiconductor heterostructure, where the conduction band profile $E_c(z)$ is engineered to create localized electronic subbands through quantum confinement.

The fundamental building blocks of this band structure are quantum wells, as illustrated in the Figure.

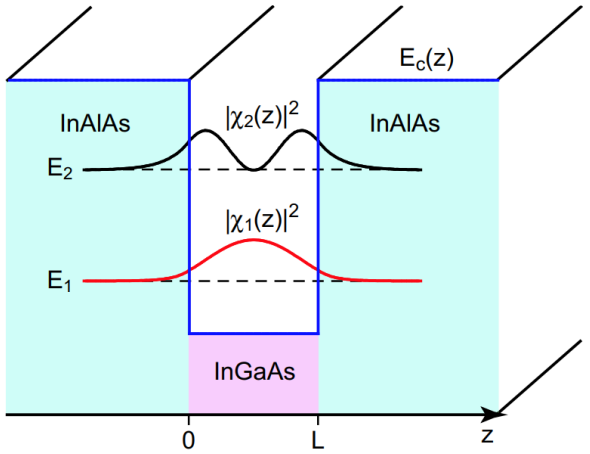

The simplest way to understand the operating principle of a quantum cascade laser is to consider a single quantum well confined between two barriers.

As an example, we consider an AlGaAs quantum well with a thickness of 7 nm and barrier height of 300 meV.

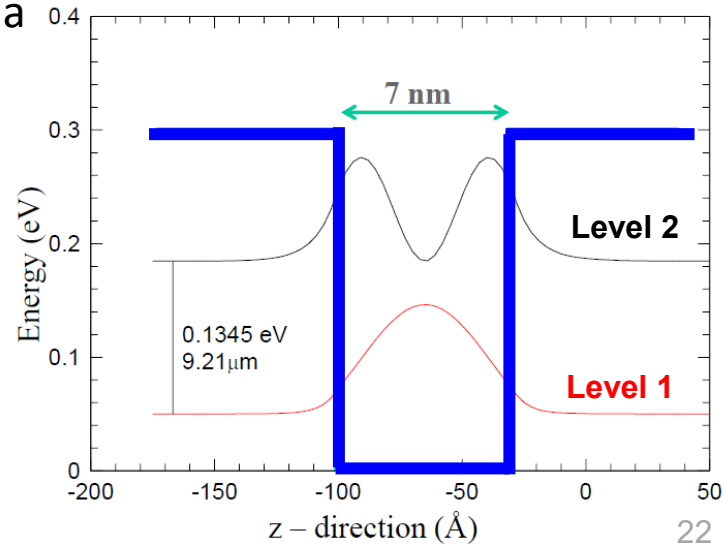

By solving the Schroedinger equation, we can calculate the **energy levels** and **wavefunctions** in the potential well.

3.2 QUANTUM CASCADE LASERS

3.2.3 From the cascade scheme to the quantum cascade laser

Starting from a single quantum well, we construct a periodic sequence of identical wells and barriers (**multiple quantum well**).

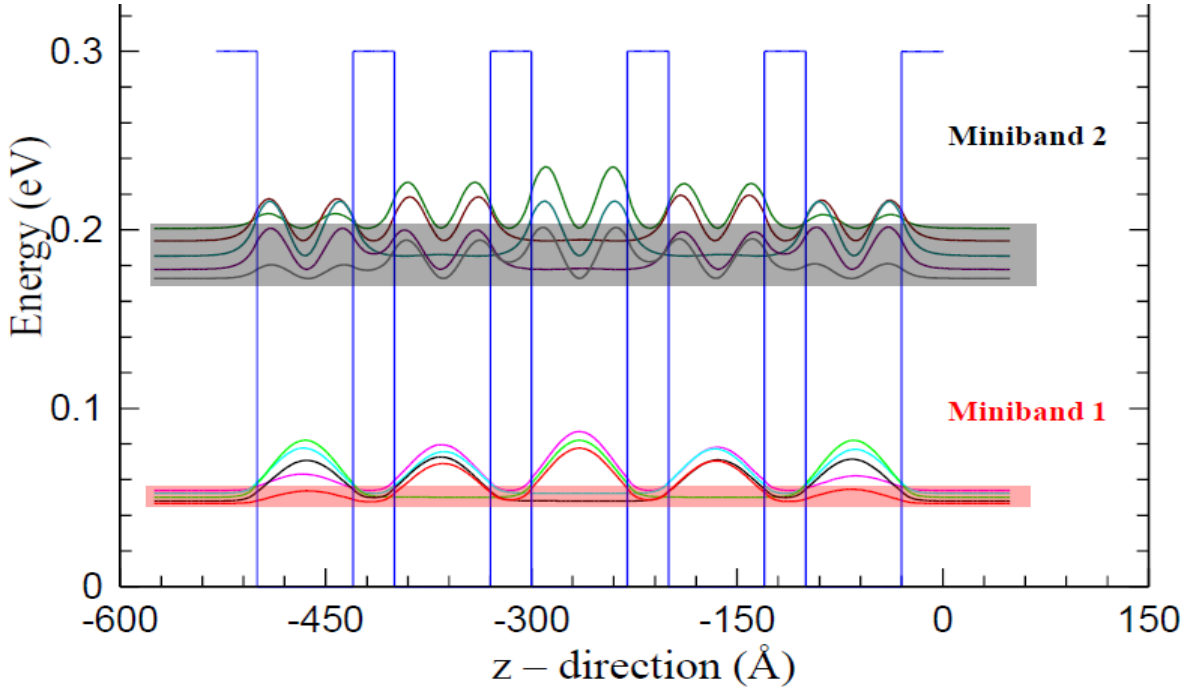

The Figure shows a periodic structure composed of 5 identical quantum wells.

Due to the coupling between adjacent wells, the wavefunctions overlap and the **discrete energy levels broaden into minibands**.

3.2 QUANTUM CASCADE LASERS

3.2.3 From the cascade scheme to the quantum cascade laser

Let's apply an **external electric field** to the multiple quantum well structure.

In the Figure, a potential drop of about 50 meV per stage (corresponding to ~40 kV/cm) is applied across the structure.

Due to the applied electric field, the **energy levels in adjacent wells are no longer aligned**.

This misalignment reduces the overlap of the wavefunctions between neighboring wells, suppressing tunneling.

As a result, the minibands break up into localized states.

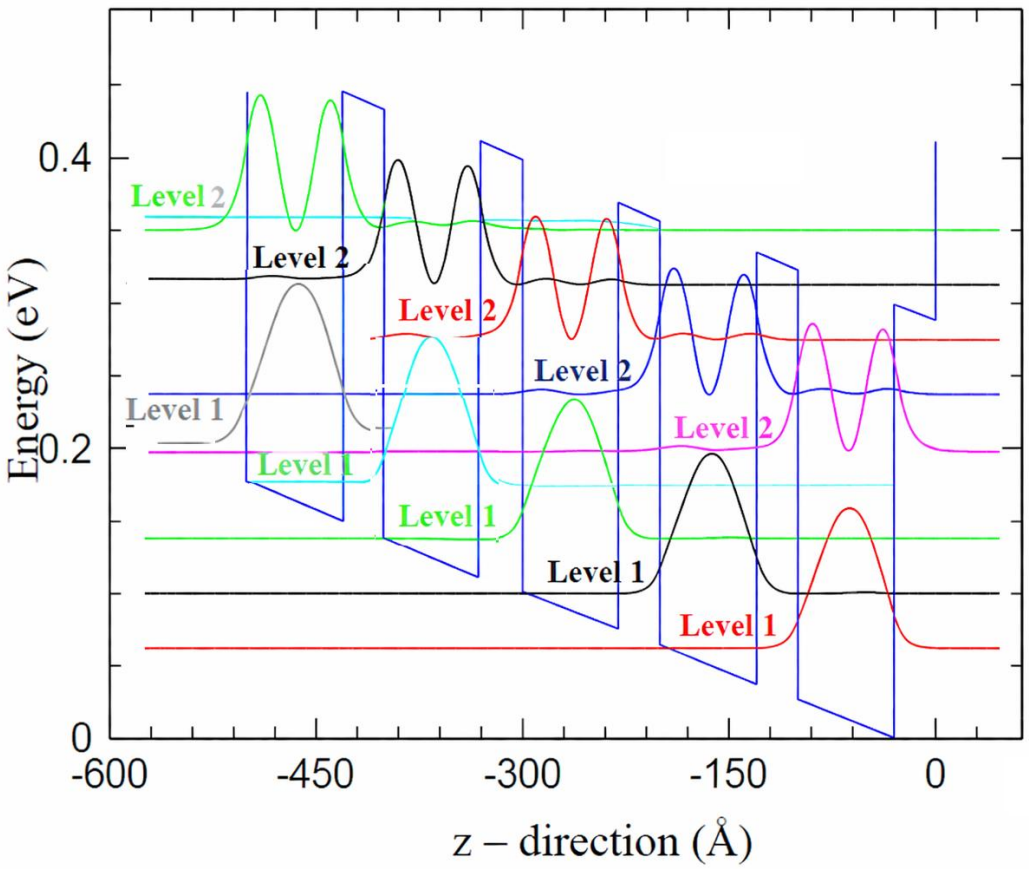

3.2 QUANTUM CASCADE LASERS

3.2.3 From the cascade scheme to the quantum cascade laser

Let's increase the applied electric field up to about 130 meV per stage.

As in Figure, **level 1 of one well is nearly aligned with level 2 of the adjacent well**, enabling sequential resonant tunneling.

To describe the **cascade process** experienced by a single injected electron, let us consider the three wells labeled **QW1**, **QW2**, and **QW3** in the Figure.

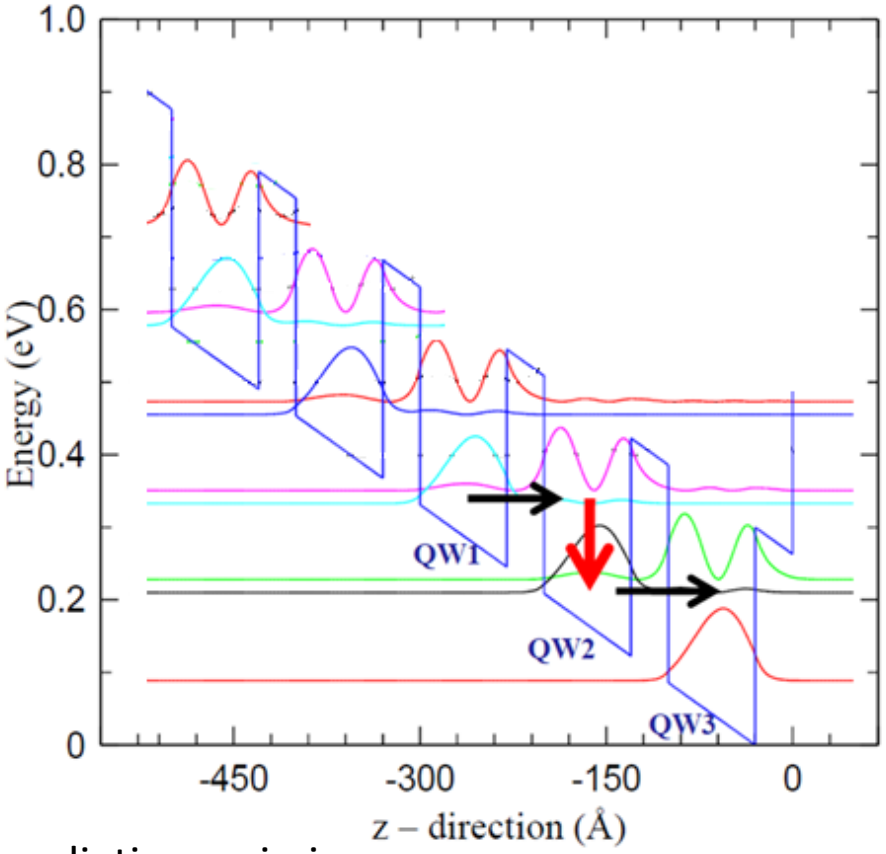

Level 1 of QW1 populates **level 2** of QW2 via resonant tunneling.

Level 2 of QW2 relaxes to **level 1** via radiative emission.

Level 1 of QW2 populates **level 2** of QW3 via resonant tunneling.

Level 2 of QW3 relaxes to **level 1** via radiative emission.

And so on... a single electron is recycled through the structure, generating multiple photons, i.e., the cascade.

3.2 QUANTUM CASCADE LASERS

3.2.3 From the cascade scheme to the quantum cascade laser

This cascade scheme highlights an important conceptual issue: in quantum wells, **subbands behave more likely as discrete energy levels**. Therefore, the problem must be reformulated in terms of population of discrete states and their occupation dynamics.

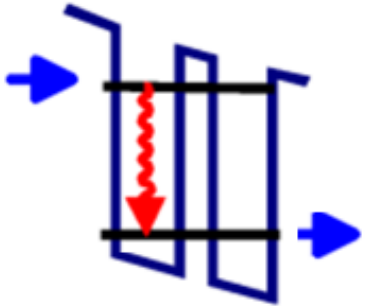

In this configuration, the **lowest subband is always populated**, making it difficult to achieve population inversion.

To achieve population inversion, it is necessary to move beyond this simple scheme and design a system with controlled level populations.

This leads to the introduction of a **three-level system**:

An **upper laser level** (population must be high)

A **lower laser level** (must be rapidly depopulated)

An **injector level** (to efficiently feed the upper state of the subsequent well structure)

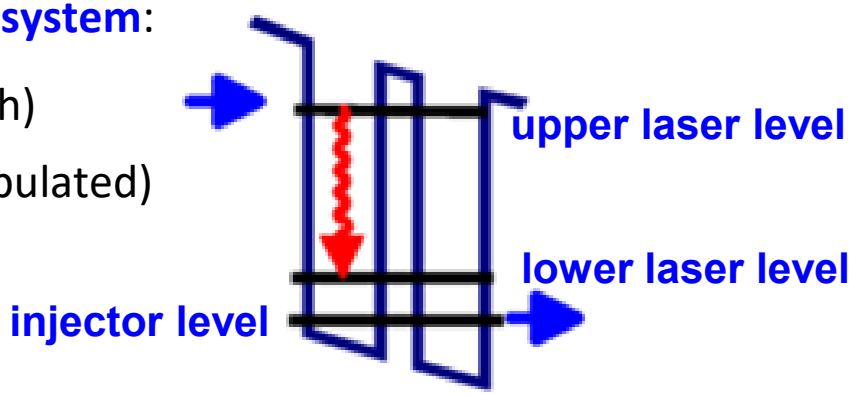

3.2 QUANTUM CASCADE LASERS

3.2.4 Electron-phonon scattering in a subband

The first crucial issue to address is: **how can we efficiently depopulate the lower laser level**?

We therefore need to analyze which scattering mechanisms can be exploited for this purpose.

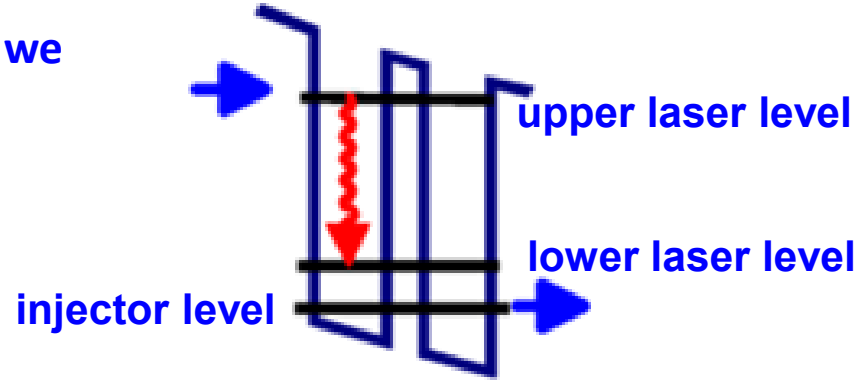

- Spontaneous emission, leading to photon emission.
- Elastic scattering due to impurities or interface roughness.
- Electron-electron scattering.
- **Electron–phonon scattering**.

Electron–phonon scattering can involve both **acoustic** and **optical phonons**.

However, acoustic phonons do not generate a macroscopic electric field, resulting in a weak interaction with electrons.

In contrast, optical phonons (LO phonons) in polar semiconductors (such as GaAs) generate **a macroscopic polarization field**.

3.2 QUANTUM CASCADE LASERS

3.2.4 Electron-phonon scattering in a subband

Since heterostructure engineering allows precise control of well and barrier thicknesses, and thus of the **subband energy separation**, the active region can be designed such that the **energy difference between the lower laser level and the injector (ground) level matches the LO-phonon energy**.

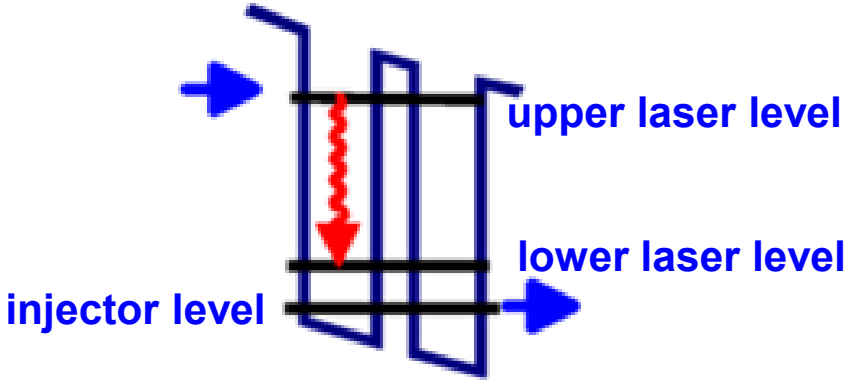

This resonance condition ensures strong coupling with LO phonons, allowing ultrafast depopulation of the lower laser level into the injector state.

A proper description of electron–phonon scattering is essential to understand its role.

At finite temperature, atoms in a crystal are not at rest but undergo thermal vibrations around their equilibrium positions.

These **collective oscillations** of the lattice can be described as phonons.

As a result, the **periodic crystal potential becomes time-dependent**, since it follows the atomic vibrations.

3.2 QUANTUM CASCADE LASERS

3.2.4 Electron-phonon scattering in a subband

However, thermal atomic vibrations are small, so the crystal potential is weakly perturbed.

In this regime, the solutions of the Schrödinger equation can be expressed as small perturbations of the unperturbed electronic states. This justifies the use of **first-order perturbation theory for electron–phonon interactions**.

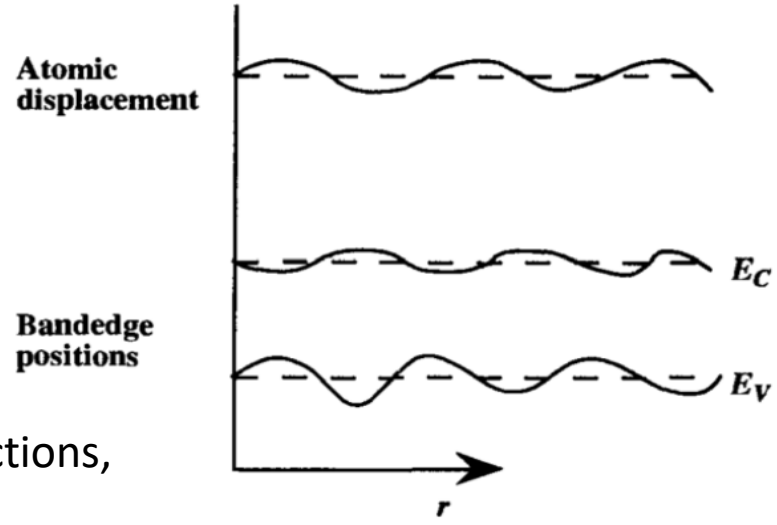

These distortions give rise to electron–phonon interactions, enabling transitions between electronic states.

In polar semiconductors, this interaction is dominated by the **Fröhlich interaction**, which arises from **the macroscopic polarization** associated with optical phonons.

The lattice vibration induces a displacement of charges, generating a polarization field:

$$\vec{P} = e(\vec{x} - \vec{y})\frac{N}{V}e^{i(\vec{q}\cdot\vec{r}-\omega_q t)}$$

where $e(\vec{x} - \vec{y})$ represents the electric dipole moment, $\frac{N}{V}$ is the carrier density in the semiconductor, and the lattice vibration associated with the phonon is described as a planewave with wave vector $\vec{q}$.

3.2 QUANTUM CASCADE LASERS

3.2.4 Electron-phonon scattering in a subband

$$\vec{P} = e(\vec{x} - \vec{y})\frac{N}{V}e^{i(\vec{q}\cdot\vec{r}-\omega_q t)}$$

The charge density associated with the polarization field can be calculated using the standard relation $\rho(\vec{r},t) = -\vec{\nabla}\cdot\vec{P}$. Since the only dependence is on the variable $\vec{r}$:

$$\rho(\vec{r},t) = -\vec{\nabla}_r\cdot\vec{P} = -e\frac{N}{V}i\vec{\nabla}_r\cdot(\vec{x}-\vec{y})e^{i(\vec{q}\cdot\vec{r}-\omega_q t)} = -e\frac{N}{V}i\vec{q}\cdot(\vec{x}-\vec{y})e^{i(\vec{q}\cdot\vec{r}-\omega_q t)}$$

The induced electrostatic potential V_q can then be obtained from Poisson's equation:

$$\nabla^2 V = -\frac{\rho}{\varepsilon}$$

Let us replace the expression we found for $\rho(\vec{r},t)$:

$$\nabla^2 V_q = \frac{e\,N}{\varepsilon\,V}\,i\,\vec{q}\cdot(\vec{x}-\vec{y})\,e^{i(\vec{q}\cdot\vec{r}-\omega_q t)}$$

We seek a solution of the form:

$$V_q(\vec{r},t) = A\,e^{i(\vec{q}\cdot\vec{r}-\omega_q t)}$$

Therefore:

$$\nabla^2 V_q = -q^2 A e^{i(\vec{q}\cdot\vec{r}-\omega_q t)}$$

3.2 QUANTUM CASCADE LASERS

3.2.4 Electron-phonon scattering in a subband

$$\nabla^2 V_q = \frac{e}{\varepsilon}\frac{N}{V}\, i\,\vec{q}\cdot(\vec{x}-\vec{y})\, e^{i(\vec{q}\cdot\vec{r}-\omega_q t)}$$

$$\nabla^2 V_q = -q^2 A e^{i(\vec{q}\cdot\vec{r}-\omega_q t)}$$

$$V_q(\vec{r},t) = A\, e^{i(\vec{q}\cdot\vec{r}-\omega_q t)}$$

By equating the first two expressions:

$$-q^2 A = \frac{e}{\varepsilon}\frac{N}{V}\, i\,\vec{q}\cdot(\vec{x}-\vec{y})$$

we obtain an expression for A :

$$A = -\frac{e}{\varepsilon}\frac{N}{V}\frac{i}{q}\overrightarrow{u_q}\cdot(\vec{x}-\vec{y})$$

where $\vec{u}_q$ is the unit vector in the direction of the wavevector $\vec{q}$.

By substituting this expression into $V_q(\vec{r},t)$:

$$V_q(\vec{r},t) = -e\frac{N}{\varepsilon V}\frac{i}{q}\overrightarrow{u_q}\cdot(\vec{x}-\vec{y})\, e^{i(\vec{q}\cdot\vec{r}-\omega_q t)}$$

This $1/q$ dependence highlights the long-range nature of the electron–phonon interaction in polar semiconductors.

3.2 QUANTUM CASCADE LASERS

3.2.4 Electron-phonon scattering in a subband

$$V_q(\vec{r},t) = -e\frac{N}{\varepsilon V}\frac{i}{q}\overrightarrow{u_q}\cdot(\vec{x}-\vec{y})\,e^{i(\vec{q}\cdot\vec{r}-\omega_q t)}$$

Let's assume that the initial $\vec{k}$ and final electronic state $\vec{k}'$ are expressed as a Bloch function in the form of $u_{\vec{k}}(\vec{r})e^{i\vec{k}\cdot\vec{r}}$ and $u_{\overrightarrow{k'}}(\vec{r})e^{i\overrightarrow{k'}\cdot\vec{r}}$, respectively:

The transition matrix elements describing the interaction between an initial electronic state $\vec{k}$ and a final state $\vec{k}'$ can then be evaluated as:

$$\langle \vec{k}|-eV_q(\vec{r})|\overrightarrow{k'}\rangle = -e\frac{N}{\varepsilon V}\frac{\mathrm{i}}{q}\overrightarrow{u_q}\cdot(\vec{x}-\vec{y})\int d\vec{r}\,u^*_{\overrightarrow{k'}}(\vec{r})u_{\vec{k}}(\vec{r})e^{i\left(\vec{q}+\vec{k}-\overrightarrow{k'}\right)\cdot\vec{r}}$$

The Fermi golden rule for intersubband scattering gives the transition rate:

$$\frac{1}{\tau_{if}} = \frac{2\pi}{\hbar}\left|\langle \vec{k}|-eV_q(\vec{r})|\overrightarrow{k'}\rangle\right|^2\delta\left(E_f - E_i + \hbar\omega_{LO}\right) \propto \frac{1}{q^2}$$

The **electron–phonon scattering rate** associated with the Fröhlich-like interaction is proportional to $\mathbf{1/q^2}$.

3.2 QUANTUM CASCADE LASERS

3.2.4 Electron-phonon scattering in a subband

$$\frac{1}{\tau_{if}} = \frac{2\pi}{\hbar}\left|\langle \vec{k}\left|-eV_q(\vec{r})\right|\overrightarrow{k'}\rangle\right|^2 \delta\left(E_f - E_i + \hbar\omega_{LO}\right) \propto \frac{1}{q^2}$$

Therefore, the interaction is **strongest for small phonon wavevectors**, i.e., near the Γ-point of the Brillouin zone. This corresponds to long-wavelength LO phonons ($q \to 0$).

As a consequence, intersubband transitions are predominantly governed by **electron–phonon scattering** rather than radiative processes.

For an electron in an excited subband, emission of an optical phonon is always allowed and leads to **excited-state lifetimes on the order of 1 ps**.

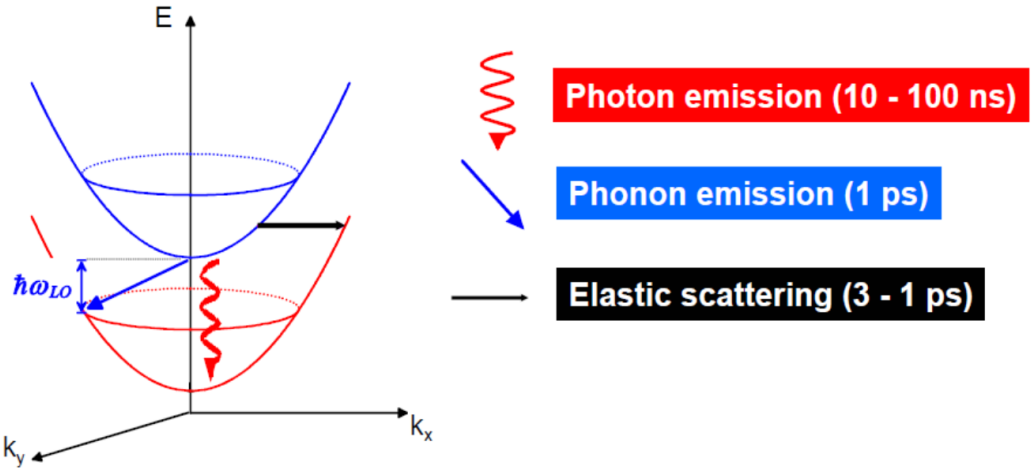

This process is generally the dominant scattering mechanism, even in high-quality heterostructures with few defects.

3.2 QUANTUM CASCADE LASERS

3.2.5 Population inversion between two subbands

Since electrons predominantly relax via spontaneous emission of optical phonons, intersubband transitions are intrinsically inefficient photon emitters.

The **radiative efficiency** is expressed as:

$$\eta = \frac{\frac{1}{\tau_r}}{\frac{1}{\tau_r} + \frac{1}{\tau_{nr}}} \sim 10^{-4} - 10^{-5}$$

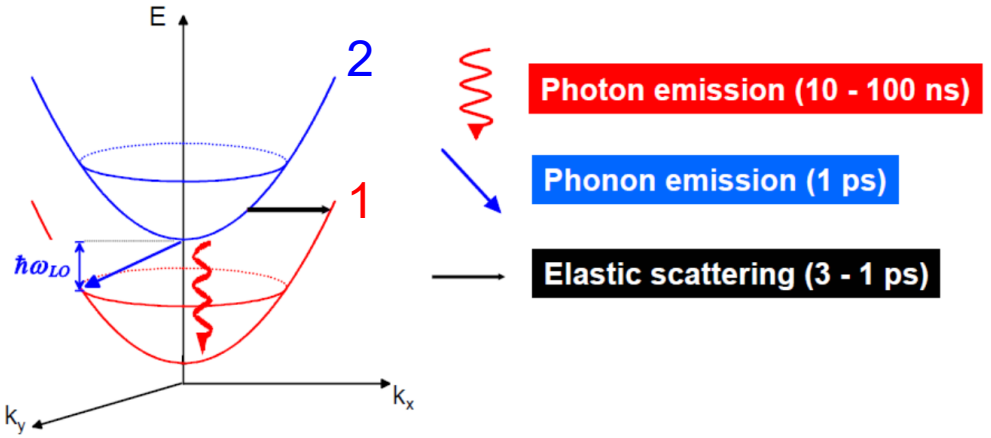

This means that if the energy separation between subband 2 and subband 1 at the Γ-point is comparable to the LO-phonon energy, the depopulation of subband 2 will predominantly occur via phonon scattering, i.e., through a non-radiative process.

Thus, a necessary (but not sufficient) condition to enhance the radiative transition $2 \rightarrow 1$ is to engineer the heterostructure such that:

$$E_2 - E_1 > \hbar\omega_{LO}$$

3.2 QUANTUM CASCADE LASERS

3.2.5 Population inversion between two sub-bands

However, the key guideline is to design a **three-level system**. In this case, the fast phonon scattering mechanism can be exploited to efficiently depopulate the lower laser level.

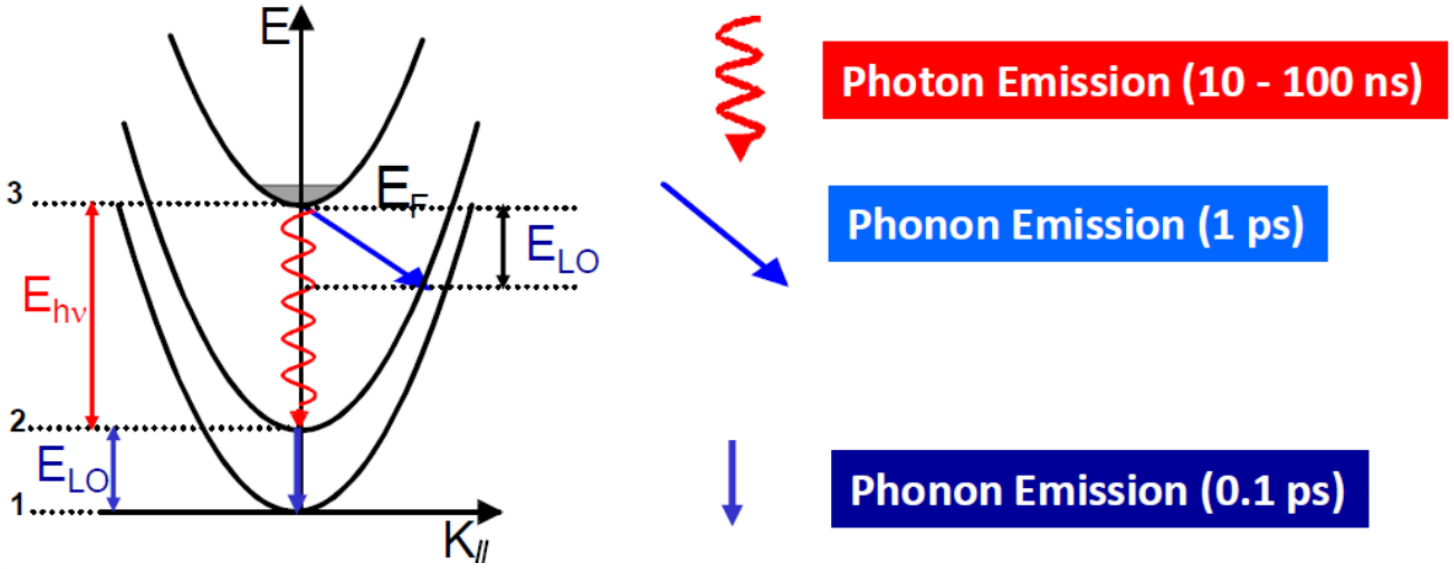

The $2 \rightarrow 1$ transition is resonant with the LO-phonon energy $E_{LO} = \hbar\omega_{LO}$, enabling ultrafast optical phonon emission with lifetimes on the order of 0.1 ps.

However, to achieve optical gain, population inversion between levels 3 and 2 is required, i.e., $\mathbf{n_3 > n_2}$.

3.2 QUANTUM CASCADE LASERS

3.2.5 Population inversion between two subbands

$n_3 > n_2$

This condition can be expressed in terms of the lifetimes of the relevant transitions:

$$\frac{n_3}{n_2} \approx \frac{\tau_{32}}{\tau_{21}} > 1$$

$$\frac{1}{\tau_{if}} \propto \frac{1}{q_{if}^2}$$

The population inversion mechanism can be understood by analyzing the Figure. The energy spacing between subbands 3 and 2 exceeds the LO-phonon energy, while the spacing between subbands 2 and 1 is comparable to $\hbar\omega_{LO}$.

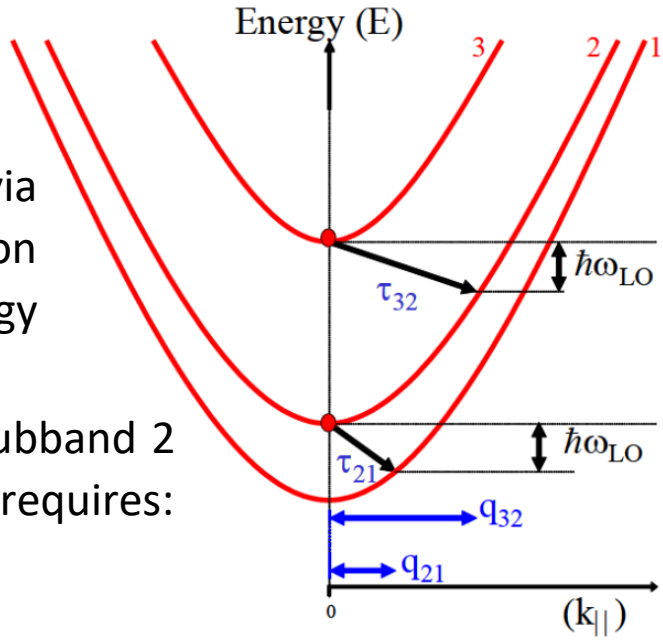

By assuming that the $3 \rightarrow 2$ transition occurs via phonon scattering, the expression for the phonon wavevector q_{32} can be derived by combining energy and momentum conservation.

When an electron relaxes from subband 3 to subband 2 by emitting an LO phonon, energy conservation requires:

$$E_3 = E_2 + \hbar\omega_{LO} + E_k$$

where $\hbar\omega_{LO}$ is the phonon energy and E_k is the residual kinetic energy of the electron in the plane.

3.2 QUANTUM CASCADE LASERS

3.2.5 Population inversion between two subbands

$$E_3 = E_2 + \hbar\omega_{LO} + E_k$$

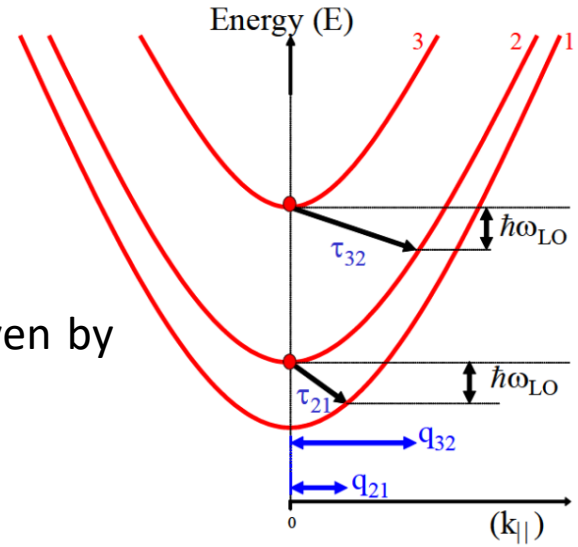

This shows that part of the energy difference is transferred to the phonon, while the remaining energy is converted into in-plane kinetic energy.

The kinetic energy associated with the in-plane motion is given by the parabolic dispersion:

$$E_k = \frac{\hbar^2 k_{32}^2}{2m^*}$$

By combining the two expressions, we obtain:

$$\frac{\hbar^2 k_{32}^2}{2m^*} = E_3 - E_2 - \hbar\omega_{LO}$$

Momentum conservation requires that the phonon carries away the in-plane momentum of the electron, $\overrightarrow{k_{32}} = \overrightarrow{q_{32}}$. Substituting $k_{32} = q_{32}$, we obtain:

$$q_{32} = \sqrt{\frac{2m^*(E_3 - E_2 - \hbar\omega_{LO})}{\hbar^2}}$$

3.2 QUANTUM CASCADE LASERS

3.2.5 Population inversion between two subbands

$$q_{32} = \sqrt{\frac{2m^*(E_3 - E_2 - \hbar\omega_{LO})}{\hbar^2}}$$

$$q_{21} = \sqrt{\frac{2m^*(E_2 - E_1 - \hbar\omega_{LO})}{\hbar^2}}$$

$$\frac{n_3}{n_2} \approx \frac{\tau_{32}}{\tau_{21}}$$

The same relation can be obtained for the phonon-assisted transition from subband 2 to subband 1.

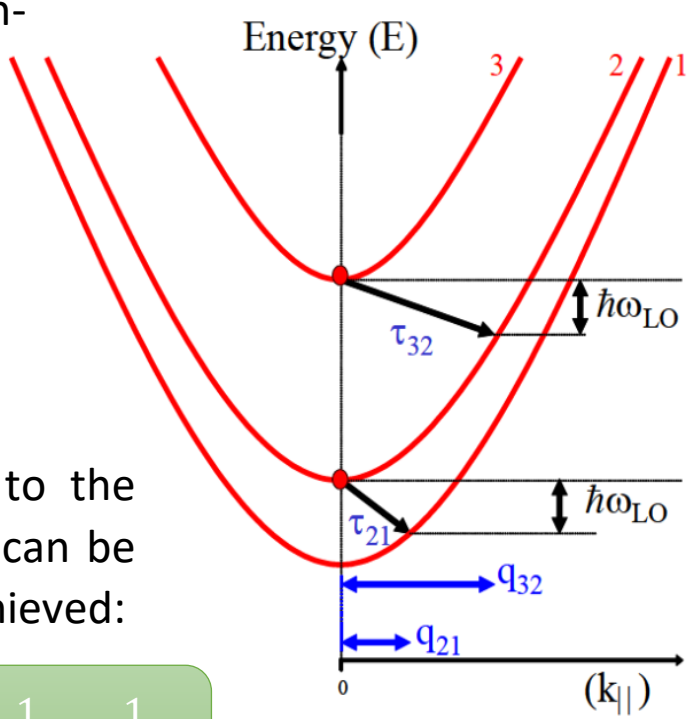

As can be seen from the Figure, since the transition 2 → 1 is almost vertical, the following relationship between phonon wavevectors is always verified:

$$q_{32} > q_{21}$$

Since the relaxation rates are proportional to the inverse square of the phonon wavevector, it can be verified that population inversion is always achieved:

$$\frac{n_3}{n_2} \approx \frac{\tau_{32}}{\tau_{21}} \approx \frac{q_{32}^2}{q_{21}^2} > 1$$

$$\frac{1}{\tau_{if}} \propto \frac{1}{q_{if}^2}$$

3.2 QUANTUM CASCADE LASERS

3.2.6 3-Level Active Region

As discussed, the cascade scheme relies on two main mechanisms:

1. **Carrier injection** into level 3 via tunneling.
2. **Radiative transition** $3 \rightarrow 2$, followed by rapid depopulation of level 2 via resonant LO-phonon scattering to level 1.

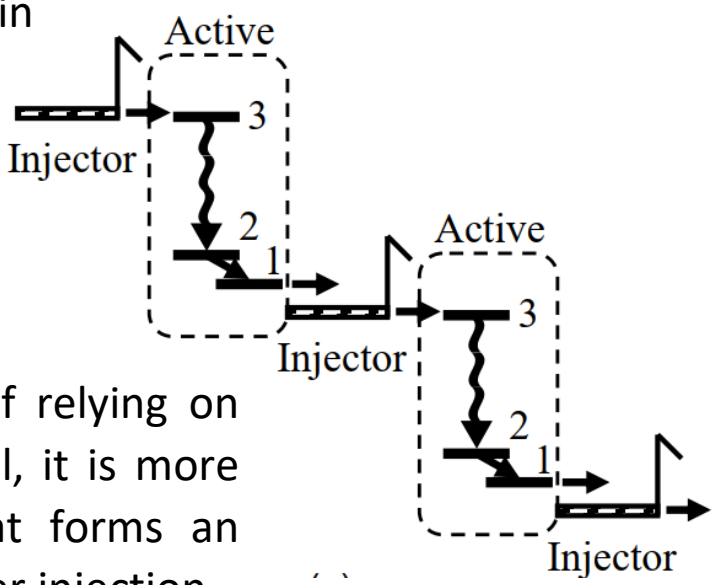

To maximize carrier injection into level 3, instead of relying on alignment with the ground level of the previous well, it is more effective to design an *ad hoc* heterostructure that forms an **injector miniband**, ensuring much more efficient carrier injection.

This defines the two fundamental building blocks of a quantum cascade structure:

1. An **injection region**, where the sequence of thin wells and barriers is engineered to form an injector miniband, which remains relatively robust even in the presence of an applied electric field.
2. An **active region**, where a different sequence of wells and barriers is designed to create the three energy levels required for laser operation.

3.2 QUANTUM CASCADE LASERS

3.2.6 3-Level Active Region

The active region is not formed by a single well, but by a tailored sequence of wide wells and thin barriers, enabling precise control of the energy level spacing.

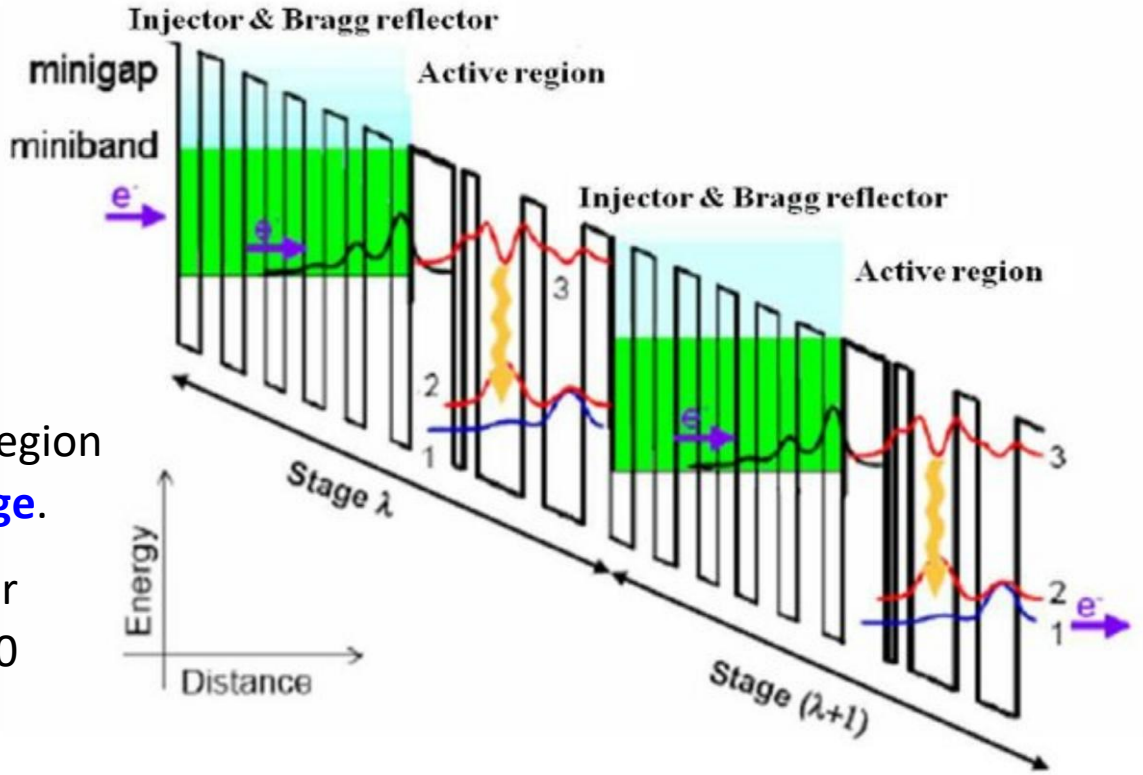

The combination of an injection region and an active region defines a **stage**.

A quantum cascade laser typically consists of 20–100 such stages.

A QCL is built from repeated stages, each consisting of an injector region (miniband) and an active region (engineered levels for lasing).

Each electron can emit one photon per stage, leading to **high optical efficiency**.

3.2 QUANTUM CASCADE LASERS

3.2.6 3-Level Active Region

A clear understanding of QCL design can be obtained by considering a simplified model in which the active region energy levels are treated as discrete (atomic-like) states.

The active region is modeled as a **three-level system**, with lasing occurring between levels 3 and 2. The injection region is described as a miniband with a constant population n_3, aligned with the upper level of the next stage.

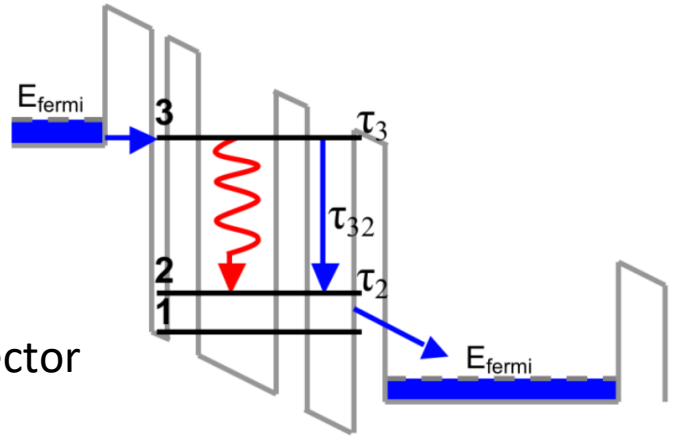

Electrons are injected into level 3 from the injector ground state of the previous period at a rate J/e.

Electrons can relax from level 3 to levels 2 and 1 with rates $1/\tau_{32}$ and $1/\tau_{31}$ respectively, or escape from the active region with rate $1/\tau_{esc}$.

The **total lifetime of level 3** is therefore:

$$\frac{1}{\tau_3} = \frac{1}{\tau_{32}} + \frac{1}{\tau_{31}} + \frac{1}{\tau_{esc}}$$

Usually, the transition rate $\frac{1}{\tau_{31}}$ is negligible by design.

3.2 QUANTUM CASCADE LASERS

3.2.6 3-Level Active Region

The injection efficiency is defined as the ratio between the current injected into level 3 and the total current:

$$\eta_i = \frac{J_3}{J}$$

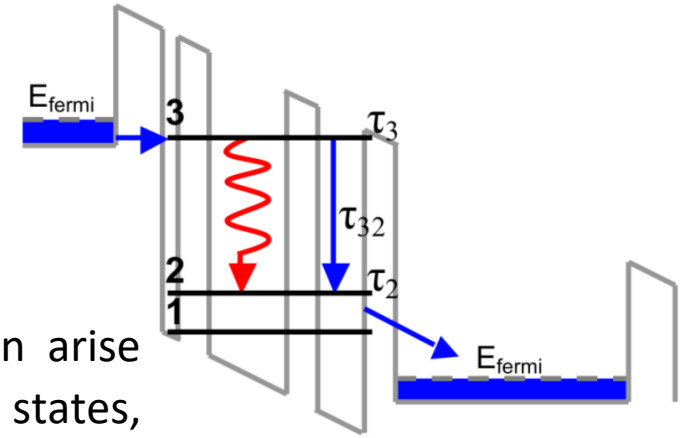

In the ideal case, $\eta_i = 1$. Deviations from this condition arise from thermal excitation into continuum or higher-energy states, as well as from parasitic injection into the lower levels (2 and 1).

We assume ideal injection into level 3 and negligible thermal population of level 2.

The population dynamics of levels 3 and 2 can be described by the following rate equations in steady state:

$$\frac{dn_3}{dt} = \frac{J}{e} - \frac{n_3}{\tau_3} = 0$$

$$\frac{dn_2}{dt} = \frac{n_3}{\tau_{32}} - \frac{n_2}{\tau_2} = 0$$

3.2 QUANTUM CASCADE LASERS

3.2.6 3-Level Active Region

$$\frac{dn_3}{dt} = \frac{J}{e} - \frac{n_3}{\tau_3} = 0$$

$$\frac{dn_2}{dt} = \frac{n_3}{\tau_{32}} - \frac{n_2}{\tau_2} = 0$$

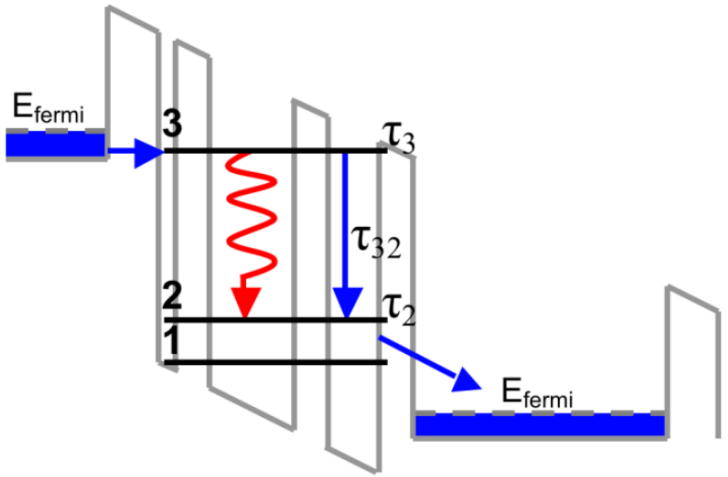

From these equations, we obtain:

$$n_3 = \frac{J\tau_3}{e}$$

$$n_2 = \frac{\tau_2}{\tau_{32}} n_3$$

The population inversion is then:

$$\Delta n = n_3 - n_2 = \frac{J\tau_3}{e}\left(1 - \frac{\tau_2}{\tau_{32}}\right) = \frac{J\tau_{eff}}{e}$$

where $\tau_{eff} = \tau_3\left(1 - \frac{\tau_2}{\tau_{32}}\right)$ is an **effective lifetime** linking population inversion to the injected current.

Note that population inversion is achieved only if $\tau_2 < \tau_{32}$.

3.2 QUANTUM CASCADE LASERS

3.2.7 Threshold current

To evaluate the optical gain in the active region of a quantum cascade laser, let us use a **phenomenological approach** starting from the device g

Consider an electromagnetic plane wave propagating along the heterostructure, which has refractive index n, thickness L_p, and width w, and contains a single three-level period.

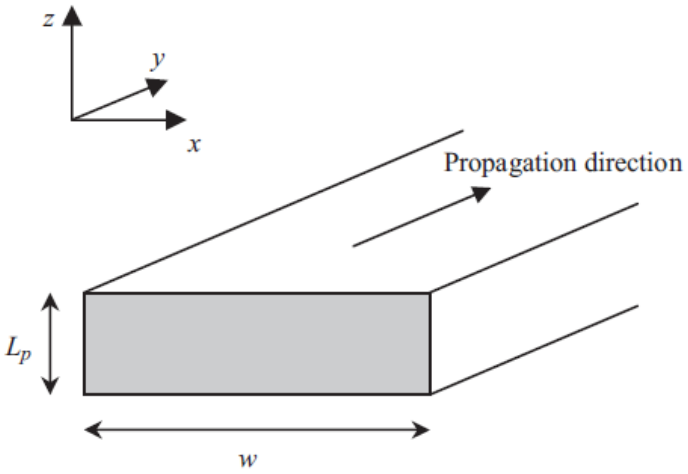

The power density carried by a **plane wave** of amplitude E_0 is given by the Poynting vector:

$$P = \frac{1}{2}\varepsilon_0 n c E_0^2$$

The **photon flux** is defined as the number of photons per unit time crossing the heterostructure cross-section of area wL_p:

$$\Phi = \frac{1}{2}\varepsilon_0 n c E_0^2 \frac{wL_p}{\hbar\omega}$$

3.2 QUANTUM CASCADE LASERS

3.2.7 Threshold current

Let us consider photons resonant with the transition between levels 3 and 2, i.e., $\hbar\omega = E_3 - E_2$.

The variation of the photon flux over an infinitesimal distance dy is given by the difference between stimulated emission and absorption processes:

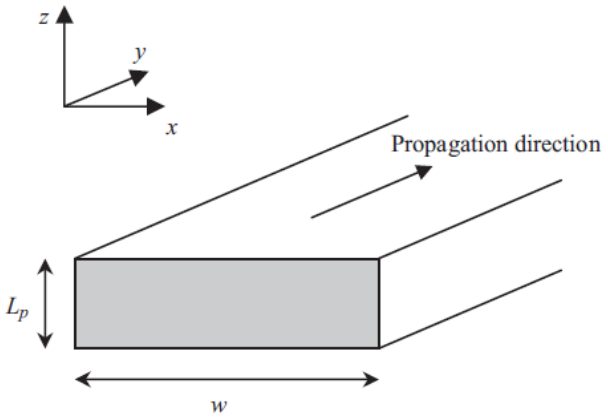

$$d\Phi = W_{32}^{max} n_3 w dy - W_{32}^{max} n_2 w dy$$

where n_3 and n_2 are the electron densities in levels 3 and 2, $W_{32}^{\max}$ is the stimulated transition rate (equal to the absorption rate), and wdy is the interaction volume.

The propagation gain is defined as the variation of photon flux with respect to the instantaneous number of photons in the cavity:

$$G = \frac{\frac{d\Phi}{dy}}{\Phi}$$

Using the previous expression: $\frac{d\Phi}{dy} = W_{32}^{max}(n_3 - n_2)w$

3.2 QUANTUM CASCADE LASERS

3.2.7 Threshold current

$$G = \frac{\frac{d\Phi}{dy}}{\Phi}$$

$$\Phi = \frac{1}{2}\varepsilon_0 ncE_0^2 \frac{wL_p}{\hbar\omega}$$

$$\frac{d\Phi}{dy} = W_{32}^{max}(n_3 - n_2)w$$

Substituting the previous expressions, we obtain:

$$G = \frac{W_{32}^{max}(n_3 - n_2)w}{\frac{1}{2}\varepsilon_0 ncE_0^2 \frac{wL_p}{\hbar\omega}} = \frac{2\hbar\omega}{\varepsilon_0 ncE_0^2 L_p} W_{32}^{max}(n_3 - n_2)$$

The transition rate W_{32}^{max} is proportional to the square of the dipole matrix element of the intersubband transition and to E_0^2. Therefore, the dependence on E_0^2 cancels out, making the gain independent of the optical field intensity.

Positive gain is achieved only if $\boldsymbol{n_3 > n_2}$, a condition that is ensured in QCLs by design.

The gain can be enhanced by optimizing the wavefunction overlap, thereby increasing the dipole matrix element.

3.2 QUANTUM CASCADE LASERS

3.2.8 Advantages of quantum cascade lasers

- **Unipolarity**

Only electrons participate in transport and emission, eliminating hole-related losses. The emission energy is controlled by quantum confinement rather than by material bandgap.

- **Cascade operation**

Each injected electron can generate multiple photons while cascading through the structure. This enables internal quantum efficiencies greater than unity and high output power.

- **Spectral Tunability**

The emission wavelength can be precisely engineered by the layer thickness and. QCLs can cover a wide spectral range from mid-infrared to terahertz (3.5-150 µm) .

- **Design flexibility**

The heterostructure allows full control of wavefunctions and energy levels. Population inversion, gain, and transport can be independently engineered .

- **Ultrafast carrier dynamics**

Carrier relaxation occurs on picosecond timescales due to strong electron–phonon coupling.